# Low Burning Rate Aluminized Propellants in Acceleration Fields

Winston N. Brundige*
*Morton Thiokol/Elkton, Maryland*
and
Leonard H. Caveny†
*Air Force Office of Scientific Research, Washington, D.C.*

**To reduce slag formation and burning rate increases, the effects of radial acceleration (up to 20 *g*) and low pressure (2-7 MPa) on the combustion of low-burning rate aluminized propellants (87 formulations) were investigated. Experiments were performed to obtain agglomerate size distribution, slag formation, and burning rate data. Data sources included photographs under cross flow and acceleration conditions, scanning electron probe (Cl and Al) images, particle collection combustors, and rocket motors. The tendency to form slag increases as the agglomeration size at the burning surface increases. A lower burning rate increases acceleration effects. However, residue formation is more sensitive to formulation than is burning rate; for example, bimodal vs trimodal AP can cause significant changes in residue in the absence of burn rate changes; RDX produces larger agglomerates than HMX. Through understanding obtained from this research, reduction in agglomeration, slag formation, and burning rate augmentation are directly attributable to systematic changes in formulation ingredient levels and sizes.**

## Introduction

OPTIMUM performance for many motors that use low-burning rate, composite, solid propellants is obtained by operating these systems at pressures below 7 MPa, and some applications require spin stabilization (generally less than 120 rpm). Research was conducted on the effects of the motor environment on the combustion of low-burn rate, aluminized, hydroxyl-terminated polybutadiene (HTPB) propellants with ammonium perchlorate (AP) and cyclotetramethylene-tetranitramine (HMX).

During combustion, agglomerates consisting primarily of molten aluminum and alumina form on the surface. The slag retention phenomenon in motors is associated with the forces acting on the agglomerates on, or adjacent to, the burning surface and with the ability of the ejected agglomerates to follow the gas streamlines. Factors such as agglomerate size and density, propellant burning rate, pressure, propellant formulation and properties (e.g., binder surface tension), motor acceleration and orientation, gas velocity in the motor port, and motor geometry determine whether agglomerate retention conditions are established.

Previous analyses and interpretations indicated that under many operating conditions the main retaining force is the surface tension of the propellant matrix.[1,2] An acceleration field in a spinning motor enhances the retention of agglomerates in the motor. However, it was uncertain whether reducing the agglomerate size under nonspin conditions would reduce the slag formation in a spinning rocket motor. Previous modeling efforts emphasized increases in burn rate due to an acceleration field that is based on retention of aluminum agglomerates.[3-7] Mechanistic models and calculations explicitly incorporated major net effects of burn rate without acceleration, acceleration level, aluminum particle size, and aluminum content. Minor effects were due to pressure, temperature, and product composition mainly as they affected the lifting capability (drag force) of the propellant gases. However, motor tests (for example, Ref. 8) have shown that slag formation can be significant in the absence of burn rate augmentation; thus, additional factors must be considered. A major theme in this research was to interpret the results in terms of understanding the combustion process.

## Experimental Approach

### Apparatus

Experiments consisted of evaluating the response of burn-rate augmentation ($r_a/r_0$) and residue (slag) formation to an acceleration field of about 12 *g* at 3.4 MPa using a slab motor based on the one developed by Northam.[9] The present configuration utilizes a slab of propellant $2.5 \times 7.6 \times 11.4$ cm. The inhibitor retains an imprint of the agglomerates remaining at burnout and was used to measure a pit density ($N_p$). Limited experiments were conducted with a particle collection bomb (PCB)[10] using an acetone/water quench liquid to obtain an indication of relative agglomerate formation tendency without an acceleration field.

Emphasis was placed on photographing and interpreting the burning of aluminized propellants under cross flow conditions similar to those that exist in rocket motors.[11] High-speed photographs were taken of agglomerates forming on the surface, moving along the surface, and entering the flowfield. Several laboratories have obtained high-resolution photographs of aluminized propellants burning as strands in quiescent atmospheres. However, to answer questions concerning agglomerate retention efficiency, the results obtained in quiescent atmospheres must be complemented by results obtained under cross flow conditions. Other investigators[2,10,12,13] have studied how formulation, pressure, and port geometry affect the size distribution of metal agglomerates under rocket motor conditions, but those investigations were not concerned with visualizing the combustion processes that produced the agglomerates.

The centrifuged window burner developed by Crowe and Willoughby[14] and located at the Naval Postgraduate School was used to visualize the agglomeration process at 12 *g* acceleration.

Presented as Paper 81-1583 at the AIAA/SAE/ASME 17th Joint Propulsion Conference, Colorado Springs, Colo., July 27-29, 1981; submitted Sept. 1, 1981; revision received April 20, 1983. 

*Scientist, Research Department. Member AIAA.
†Program Manager. Associate Fellow AIAA.

### Propellant Formulations

Eighty-seven propellant formulations were tested. The investigation emphasized the effect of formulation variables on burn rate, burn-rate augmentation, and residue in the modified slab motor at 0 and 12 *g* radial acceleration. Twenty propellants were selected for evaluation of motor parameter effects (initial temperature, pressure level, and acceleration level) in the slab motor over the ranges of −20-40° C, 1.7-6.9 MPa, and 0 to 20 *g*. The 3-kg (7-lb), spinning 127-mm (5-in.) cylindrically perforated (CP) motor provided supplemental data at 15° C; 3.4 MPa, and 0, 6, and 12 *g* radial acceleration, particularly with respect to residue (slag) formation.

The general approach for selecting specific formulations was to start with a representative HTPB propellant and then make systematic variations to that baseline emphasizing those changes found to have affected burn rate or aluminum agglomeration in various propellant systems under other programs. One variable was changed at a time, then concommitant variations were added to investigate interactions among the more important variables (for example, Al, AP, and HMX sizes and levels).

## Effect of Formulation Changes

### Aluminum Level

In general, as the aluminum level increased, the burn rate decreased slightly, the agglomerate formation in the PCB increased significantly, and the burn rate augmentation, pit density, and residue all increased rapidly (Table 1). The sensitivities to aluminum level were, as expected, based on the formation of aluminum agglomerates as the key factor in controlling sensitivity to an acceleration field; however, the large changes in percentage of agglomeration in the PCB and the amount of residue left in subscale test motors were extremely sensitive to even a 1 or 2% increase in aluminum level. This sensitivity probably reflects the fact that the propellants investigated were all in a borderline region. If one looked at the other factors, such as burn rate, burn rate augmentation changes, or percent of agglomerates greater than 75 $\mu$m, one would see changes more in line with a 10% change in the relative amount of aluminum present (i.e., an increase in level of aluminum in a formulation from 18 to 20%). The factors that are most sensitive to larger agglomerates, such as the percentages greater than 150 $\mu$m ($F_{150}$) in the PCB or the pit density ($N_p$) in the slab motor, are the ones that showed a two-fold increase for the aforementioned change in aluminum level. Thus, one is left with the impression of threshold effects. Factors favoring efficient combustion, such as the removal of all 400 $\mu$m AP, shifted the area of investigation to a regime removed from the threshold area and thus lowered the sensitivity to changes in aluminum level.

### Binder Level

Increasing binder level significantly lowered the burn rate in most of the formulations studied. As long as the burn rate was above 0.5 cm/s at 3.4 MPa and the oxidizer to fuel ratio was above 1.1, the influence of binder level on agglomeration, burn rate augmentation, and residue was minor. However, significant changes were noted on more marginal, lower rate formulations. The data in Table 2 show the trends that resulted when the AP level was decreased as binder level was increased. Regression analyses separated the two effects so that it became apparent that the overriding factor is the decrease in the amount of AP rather than the increase in binder level. If the binder level were increased at the expense of an ingredient other than AP, such as aluminum or HMX, the net effect could be a decrease in agglomeration. Formulation of practical propellants for specific applications normally severely penalizes this kind of trade-off. However, from a mechanistic point of view, the study of binder level changes provided evidence that isolation of the aluminum particles by additional binder during the initial heating of the surface may have actually reduced agglomeration. This effect did not carry over into the formation of pits and burn-rate augmentaton; in which case, the pit density in the slab motor increased significantly as the binder content increased. This implies that the isolating effect of the binder that decreased agglomeration also decreased the ratio of lift to retention forces for those agglomerates that were still formed. Thus, it is possible that a propellant can form fewer agglomerates, but those agglomerates are less likely to be entrained in the flowfield.

**Table 1 Aluminum level variation**

| Al, % | Slab motor $r_0$, cm/s | $r_a/r_0$ | $N_p$, pits/cm$^2$ | PCB $F_{75}$, % | $F_{150}$, % |
|---|---|---|---|---|---|
| 18 | 0.600 | 1.06 | 1.7 | 90 | 36 |
| 20 | 0.579 | 1.10 | 2.6 | 92 | 57 |
| 22 | 0.564 | 1.11 | 3.4 | 95 | 64 |

**Table 2 Binder level variation**

| Binder, % | Slab Motor $r_0$, cm/s | $r_a/r_0$ | $N_p$, pits/cm$^2$ | PCB $F_{75}$, % | $F_{150}$, % |
|---|---|---|---|---|---|
| 10 | 0.627 | 1.05 | 0.7 | 89 | 35 |
| 11 | 0.600 | 1.06 | 1.7 | 90 | 36 |
| 12 | 0.574 | 1.13 | 2.5 | 92 | 47 |
| 14 | 0.493 | 1.26 | 3.7 | 93 | 60 |

**Table 3 HMX level variation**

| HMX level, % | Slab Motor $r_0$, cm/s | $r_a/r_0$ | $N_p$, pits/cm$^2$ | PCB $F_{75}$, % | $F_{150}$, % |
|---|---|---|---|---|---|
| 0 | 0.610 | 1.08 | 1.7 | 62 | 8 |
| 10 | 0.610 | 1.02 | 0.5 | 81 | 23 |
| 20 | 0.554 | 1.12 | 3.9 | 92 | 37 |

### HMX Level

The addition of HMX decreased the burn rate and increased burn-rate augmentation and residue for a given Al and binder level. Replacing a portion of the AP with HMX made no significant change in the overall effects of aluminum, binder, or coarse AP level changes. As noted in Table 3, adding less than 20% HMX produced an unusual decrease in augmentation and pitting, even though agglomeration increased. A very sensitive balance existed, as shown by the significant increases in all measured parameters (except burn rate), when HMX was increased from 10 to 20%. The role of HMX as a low-molecular-weight gas producer appeared to outweigh its effect as a source of heat at low levels, a trend which reversed at higher levels.

### RDX

Further evidence regarding the importance of the local environment on the agglomeration and lifting of the aluminum particles was provided by substituting RDX for HMX. Since RDX decomposes at a lower temperature than HMX, it should have released its energy at the surface sooner than HMX as the regressing surface approached and passed. It has been postulated[6,7] that the Al particles accumulate in a mobile layer before entering the primary diffusion flame

leading to agglomeration prior to ignition. Additional low-heat release in this mobile layer by a material such as RDX or HMX that does not cause a decrease in the thickness of the layer tends to accentuate aluminum accumulation. Various tests indicated that, when substituted for HMX, RDX should provide a somewhat lower surface temperature for the region between the large AP particles (Fig. 1 and Table 4).

#### AP Average Particle Size

Major effects were noted due to the level of coarse AP and whether a bimodal or trimodal distribution of AP was used. As noted by Miller[15] and Osborn,[16] these effects can be summarized as a combination of the changes due to the average AP size and the width of the particle size distributions. In general, the larger the average size of the AP, the more agglomeration and the lower the burn rate. Also, the wider the distribution of the AP particle sizes, the greater the amount of agglomeration. As a result, the spin sensitivity of the propellant is often decreased by a reduction in the amount of coarse AP and the use of trimodal blends (where a middle size replaces some of the two end sizes). Much of the effect of increases in the amount of coarse AP appears to be related to decreasing the burn rate. Much of the effect of the particle distribution width appears to be on the aluminum agglomeration and its effects on spin sensitivity.

Data presented in Table 5 represent controlled variation of either the AP trimodal or AP bimodal with no change in the other parameters within a given group of propellants. The trimodal variation study, for which the only variation was the ratio of coarse to regular AP, represented a change in the average size of the AP independent of the level of fine AP. As the average size increased, the burn rate decreased in a regular fashion, and the burn-rate augmentation, pit density, PCB agglomeration, and 127-mm (5-in.) CP slag all increased in a regular fashion; that is, the change in these parameters with the change in average AP diameter was linear, while all other variables remained constant. The propellants documented in Table 5 using a bimodal distribution show trends that were a function of the amount of coarse AP in the propellant. As expected, increases in the amount of coarse AP at the expense of fine AP coincided with the trends where the average diameter of the coarse fraction was being increased (by varying 400 $\mu$m/200 $\mu$m ratio) while the fine fraction was being held constant.

The question of whether a bimodal AP distribution is inherently different from a trimodal distribution is addressed in Table 6. The two groups of propellant shown represent

**Table 4 Substitution of RDX for HMX**

| | Slab Motor | | | PCB | |
|---|---|---|---|---|---|
| Nitramine | $r_0$, cm/s | $r_a/r_0$ | $N_p$, pits/cm$^2$ | $F_{75}$, % | $F_{150}$, % |
| HMX | 0.610 | 1.02 | 0.5 | 81 | 23 |
| RDX | 0.587 | 1.10 | 1.4 | 91 | 45 |

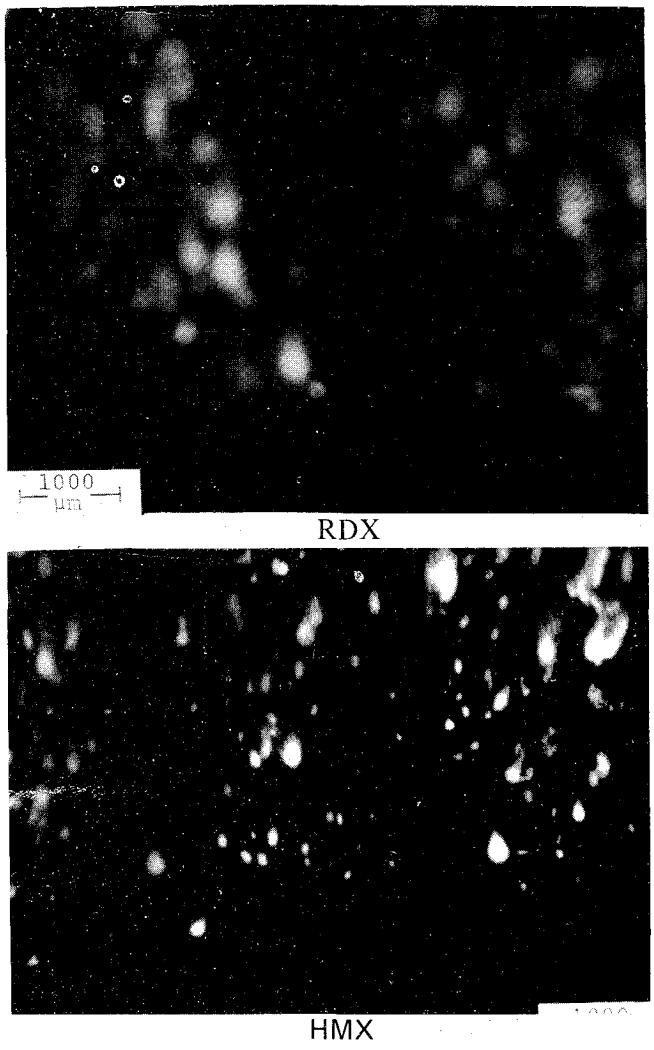


Fig. 1 Single frames from cross flow window burner films comparing RDX to HMX.

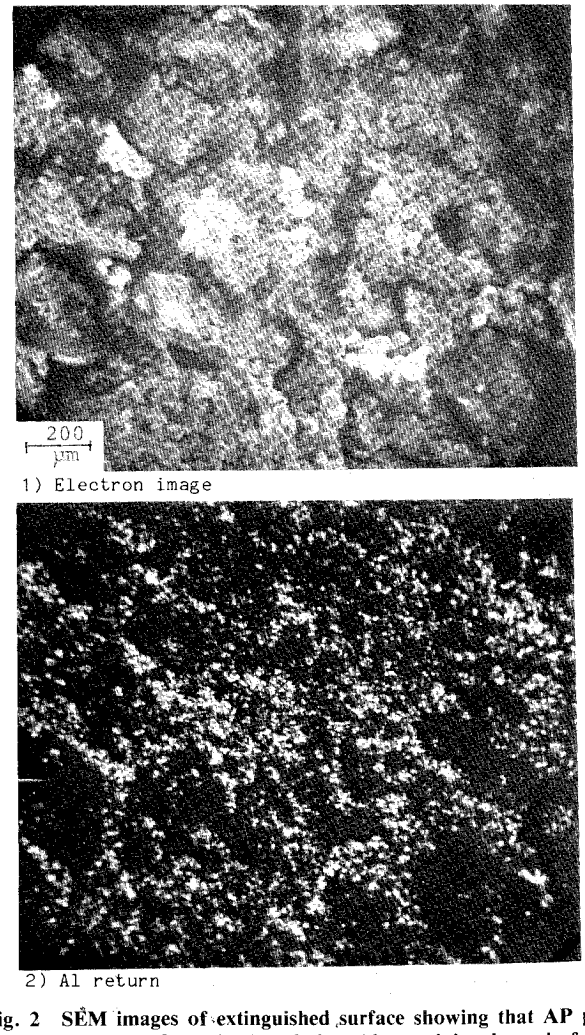


Fig. 2 SEM images of extinguished surface showing that AP particles are not clearly defined and that Al-containing layer is fairly uniform (AP/Al/HTPB baseline, 3.45 MPa).

**Table 5 Effect of changing AP modal**

| Ratio of AP | | | Slab motor | | | PCB | |
|---|---|---|---|---|---|---|---|
| 400 $\mu$ | 200 $\mu$ | Fine | $r_0$, cm/s | $r_a/r_0$ | $N_p$, pits/cm$^2$ | $F_{75}$, % | $F_{150}$, % |
| | | | AP trimodal | | | | |
| 45 | 45 | 10 | 0.620 | 1.04 | 0.5 | 87 | 23 |
| 60 | 30 | 10 | 0.600 | 1.06 | 1.7 | 90 | 36 |
| 75 | 15 | 10 | 0.564 | 1.17 | 2.8 | 94 | 59 |
| | | | AP bimodal | | | | |
| 50 | — | 50 | 0.676 | 1.03 | 0.8 | 65 | 9 |
| 60 | — | 40 | 0.587 | 1.13 | 1.7 | 85 | 29 |
| 70 | — | 30 | 0.518 | 1.21 | 3.4 | 92 | 66 |

**Table 6 Bimodal vs trimodal AP distribution**

| Ratio of AP | | | Slab motor | | | PCB | |
|---|---|---|---|---|---|---|---|
| 400 $\mu$ | 200 $\mu$ | Fine | $r_0$, cm/s | $r_a/r_0$ | $N_p$, pits/cm$^2$ | $F_{75}$, % | $F_{150}$, % |
| 70 | — | 30 | 0.640 | 1.07 | 1.7 | 73 | 2 |
| 60 | 20 | 20 | 0.620 | 1.04 | 0.3 | 85 | 24 |
| 60 | 30 | 10 | 0.600 | 1.06 | 1.7 | 90 | 36 |
| 70 | — | 30 | 0.594 | 1.07 | 2.2 | 41 | 0 |
| 60 | 20 | 20 | 0.600 | 1.05 | 1.2 | 59 | 10 |
| 60 | 30 | 10 | 0.592 | 1.02 | 0.8 | 73 | 8 |

**Table 7 Aluminum size variation**

| Al size, $\mu$m | Slab Motor | | | PCB | |
|---|---|---|---|---|---|
| | $r_0$, cm/s | $r_a/r_0$ | $N_p$, pits/cm$^2$ | $F_{75}$, % | $F_{150}$, % |
| 7 | 0.655 | 1.03 | 5 | 93 | 56 |
| 30 | 0.600 | 1.06 | 1.7 | 90 | 36 |
| 84 | 0.566 | 1.07 | 0.6 | 83 | 27 |

comparisions for which the only variation involves going from a bimodal distributon to a trimodal distribution at approximately the same average AP weight mean diameter. As the change was made from bimodal to trimodal, a regular change in properties appeared as follows: the burn rate and the burn-rate augmentation decreased very slightly and the pit density decreased even more. The greater burn rate augmentation and pit density noted with the bimodal AP distribution appear to be related to the less uniform AP distribution exposed at the surface for the bimodal, rather than for the trimodal. The result was a less uniform lifting force on the agglomerates in the bimodal distribution; thus, there was a greater tendency for the agglomerates to remain near the surface for longer periods of time, producing greater heat feedback. Regardless of observations and postulates about the lack of aluminum combustion heat feedback affecting the burn rate in higher burn rate AP propellants, the relatively low-burn rates and large, "slow-lifting" agglomerates of the propellants studied here apparently do influence the burn rate. This trend supports the Petite Ensemble Model as extended for aluminum,[16] rather than the approaches that consider aluminum merely as a heat sink. This is consistent with the greater sensitivity to acceleration of the burning process and the higher burn rate of the bimodal at the same average distribution. The higher agglomeration with the trimodal is more a function of the amount of fine material present. In the bimodal distributions tested, the large quantity of fine AP in the vicinity of the aluminum particles produced more rapid ignition and oxidation for the aluminum due to a locally more oxygen-rich environment. That is, as the total amount of fine AP increased, the burn rate increased and, in general, the augmentation, pit density, agglomeration, and residue all decreased.

### Al Size

The effect of aluminum size produced somewhat conflicting results (Table 7). The amount of agglomeration in the PCB tests was insensitive to changes in Al size above 7-$\mu$m Al, and the major difference was a decrease in burn rate that led to a slight increase in burn rate augmentation. The use of very fine (7 $\mu$m) Al produced a significant amount of agglomeration in the PCB, which resulted in a large population of fine pits in the slab motor (much finer than normally detected). Comparison of the cross flow window burner high-speed films for three of the formulations revealed a much higher number density of appreciably smaller agglomerates at higher pressures for the 7-$\mu$m Al propellant, which resolved into large individual agglomerates at 3.5 MPa (515 psia). The 84-$\mu$m Al propellant showed a paucity of individual particles, which emphasized the difference in number of particles in the original formulations.

### Agglomeration of Al

Combustion of the aluminum in these very low-burn rate propellants containing large particle size AP can be interpreted by the pseudopropellant type theory[17,18] (which considers surface layer heterogeneity) as it relates to the Crump pocket model.[16,19] A majority of the close-in flame combustion occurred in the portion of the diffusion flame controlled by the finest particles of AP present. Ignition of the aluminum particles within the pocket between the coarser AP particles tended to be very slow unless a significant amount of fine AP was blended with the aluminum within those pockets. Conditions that tended to make the combustion process more heterogeneous accentuated the tendency of the aluminum to be affected by the pocket conditions. Up to a certain point, as the surface became homogeneous with respect to the oxidizer particles, the influence of the pocket decreased. The PCB and slab motor data, supported by the window burner films, provided the basic data for making

conclusions about particle size effects. Evidence that this had to do with the agglomeration and combustion of aluminum was obtained from scanning electron microscopy studies of extinguished surfaces. The aluminum return microphotographs showed, in general, a fairly uniform distribution of the aluminum particles over the extinguished surface (Fig. 2). Even with propellants that formed significant agglomeration, the general appearance of the original aluminum particles was unchanged. This suggested accumulation of the aluminum particles so that they retained their original indentity, but were stuck to adjacent particles, similar to observations by Price,[1] Kraeutle,[20] and Gladun et al.[21] Whether this occurred during the extinguishing process or the combustion process cannot be determined from these photographs.

One propellant resulted in a coalescence of the aluminum layer in the center of the large AP particles for a portion of the covering. This permitted viewing the pockets between the 400-$\mu$m AP crystals. Comparison of the aluminum and chlorine images to the normal scanning electron microscope (SEM) photographs suggested that the fine AP had burned out in the pockets between the larger crystals, leaving behind the aluminum particles that were originally present (Fig. 3). The fine AP burned out much more rapidly than the coarser particles and exposed the aluminum to the heat feedback from the flame zone for a much longer period of time. The supposition here is that the propellant with the coalesced aluminum layer followed the same general combustion mechanism as other propellants, but it had a binder curative modification that increased the thickness of the surface

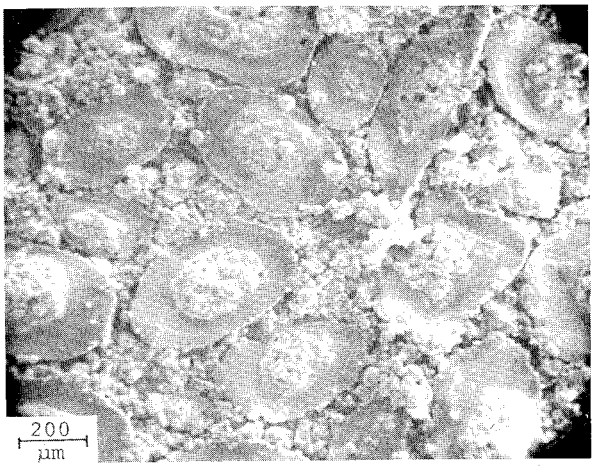


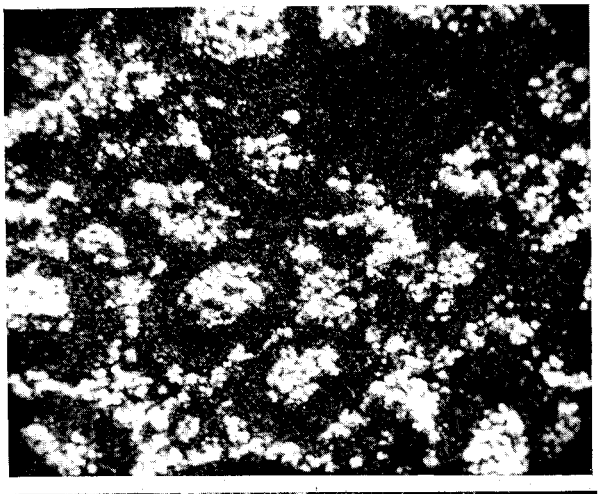

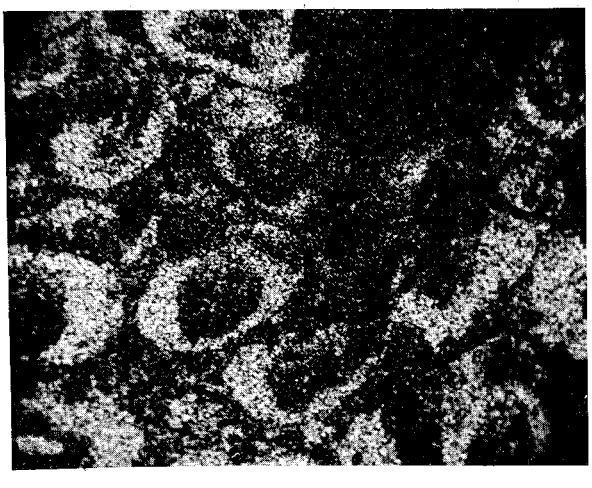

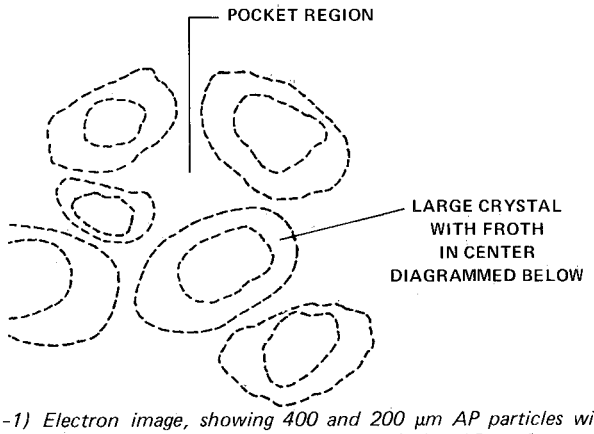


*-1) Electron image, showing 400 and 200 μm AP particles with degraded material toward the center of the AP surfaces and 30-50 μm particles between large AP crystals.*

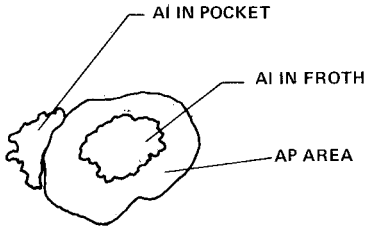


*-2) Al image, revealing that material in center of AP and between AP particles has high aluminum content. (Note that particles may be concentrating themselves as a pre-agglomeration step.)*

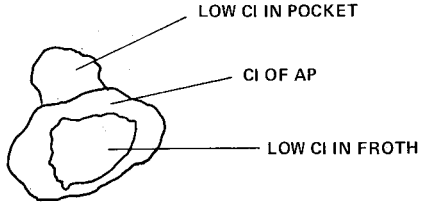


*-3) Cl image, confirming that centers of AP particles are covered with material other than AP froth and little AP remains between large particles. (Reason for lack of return from upper right corner is not known.)*

**Fig. 3 SEM images of extinguished surface examined to accentuate surface structure.**

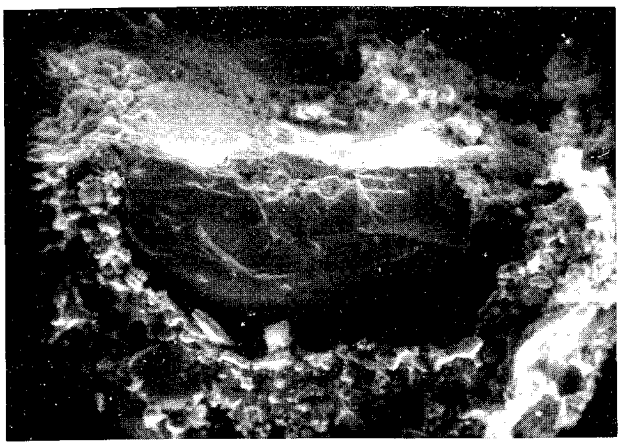


*Electron image showing cleaved single large AP crystal with residue in center and binder area below*

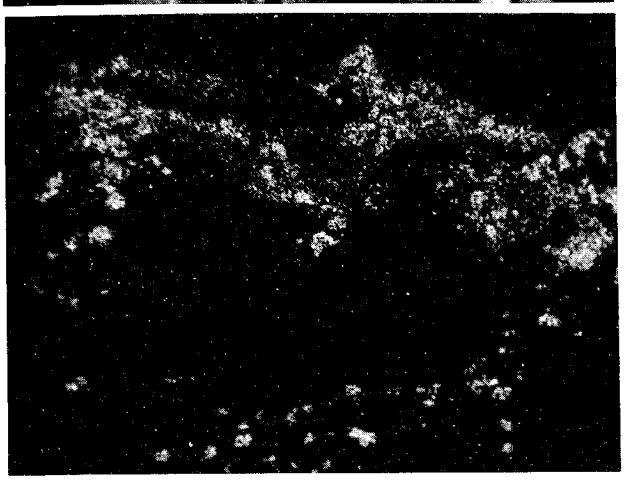


*Al image showing accumulating Al in center of AP and elsewhere on surface plus individual particles below surface*


*Cl image showing some AP over Al in center of crystal plus lack of AP surface to left of crystal*

**Fig. 4 SEM images of sectioned extinguished surface with cleaved large (400 $\mu$m) AP crystal.**

**Table 8 General trends from slab motor data**

| Parameter measured | Response of parameter as: Pressure increases, 1.7-3.4 MPa | Pressure increases, 3.4-6.5 MPa | Temperature increases, −20° − 15°C | Temperature increases, 15° − 40°C | Acceleration increases, 0-20 g |
|---|---|---|---|---|---|
| Pressure exponent | — | — | — | — | Up 0.5-1.5 %/g |
| Temp sensitivity | — | — | — | — | Down 0-2.3%/g |
| Burn rate augmentation | Up 1.5-4.5%/MPa | Up (less) 0-2.5%/MPa | Up 0-0.03%/°C | Up 0-0.3%/°C | Up 0-1%/g[a] |
| Residue | Up 15-90%/MPa | No change | No change | No change | Down 1-3%/g[b] |
| Pit density | Up 15-45%/MPa | No change | No change | Up 0.05-0.15%/°C | Up[a] |

[a] Little or no increase to 7g, sometimes decrease in $r_a/r_0$ below 7g. [b] Artifact of slab motor geometry. 5-in. CP shows expected increase as acceleration level increases.

mobile layer, allowing the aluminum near the surface to coalesce during the extinguishing process, whereas normally it did not. Exposed areas in some of the photographs from experiments with other propellants suggested that underneath the general aluminum covering, the same situation existed. However, no hard evidence could be obtained. A cross-sectional profile of the surface reveals how inadequate general conclusions can be, since the photographs clearly show an admixture of aluminum- and chlorine-containing material (Fig. 4). Thus, some microphotographs suggest that the AP has burned out in the pockets, but others suggest that it is simply masked by the aluminum mixed with it.

## Effect of Motor Environment

### Pressure, Temperature, and Acceleration Level

Slab motor tests with 20 propellants were used to develop the general trends listed in Table 8. Increases in burn-rate augmentation were noted as pressure, temperature, and acceleration level were increased. In this case, the pit density did not always increase with augmentation, suggesting that the variations in burn-rate augmentation also reflected variations in the heat feedback from the aluminum agglomerates formed. The absence of increase in residue both at higher pressures and under variations in initial propellant temperature is important in evaluating larger scale motor data, that is, some variation in pressure or conditioning temperature should not affect the slag formed.

Acceleration effects provided some interesting results. The pressure sensitivity, measured as changes in burn-rate equation exponent, increased with increasing acceleration level, but temperature sensitivity at constant surface area/throat area decreased. The burn-rate augmentation appeared to have some threshold acceleration level before increases were noted. As noted in Figs. 5 and 6, both the threshold level and the rate of increase can vary with formulation, probably defined by a combination of the amount of agglomeration and the ability to lift the agglomerates into the flowfield.

Changes in residue appeared to be largely a function of geometry. The 127-mm (5-in.) CP residues increased with acceleration level in a normal manner, but the slab motor residues actually decreased. Consideration of their respective geometries provides an insight into this effect. A compression of the flowfield in the slab test motor would result in less particle impingement on the metal wall opposite the propellant slab; thus, the residue in this test motor is decreased in centrifuge tests. In the case of a 127-mm (5-in.) CP test motor, spinning the motor would cause a regular increase in residue by compressing the flowfield toward the outer diameter and causing additional impingement on the nozzle entrance and on the head end (see Fig. 7).

### Particle Trajectory Analysis

The usefulness of drag relationships for predicting particle trajectories was examined. The cross flow window burner films provided a basis for making this evaluation for representative particles. Although some uncertainty existed concerning the absolute size of the particles, relative calculations comparing one particle to another should still be valid. The distance-time data were tabulated for approximately 100 agglomerates for a range of test conditions under approximately one-dimensional, nearly constant flow conditions. Figure 8 is a plot of the distance-time data for two agglomerates that have somewhat different responses to the flowfield. The data were taken for low cross flow velocities to allow the agglomerates to be tracked for 10 to 20 frames.

For the purpose of approximating the influence of the gas flow on the molten agglomerates, calculations of the mean gas flow properties and agglomerate behavior along the port were performed using the stagnation properties of the gas in the

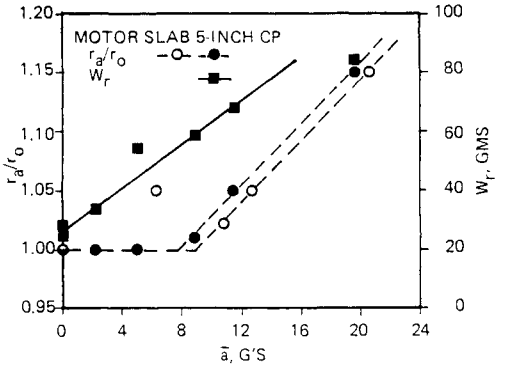


Fig. 5 Burn-rate augmentation and residue vs radial acceleration for baseline propellant.

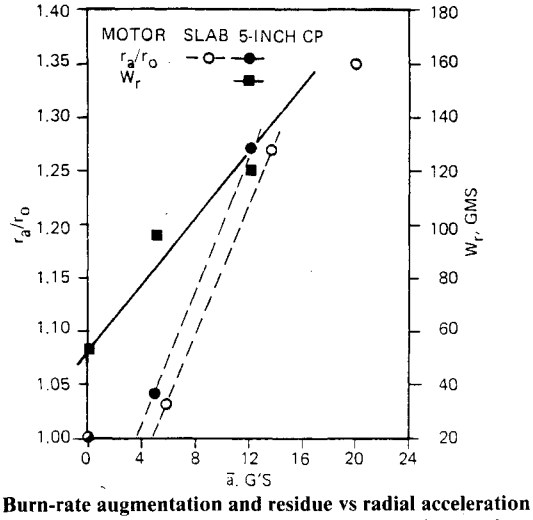


Fig. 6 Burn-rate augmentation and residue vs radial acceleration for increased acceleration sensitivity propellant (baseline with 14% binder).

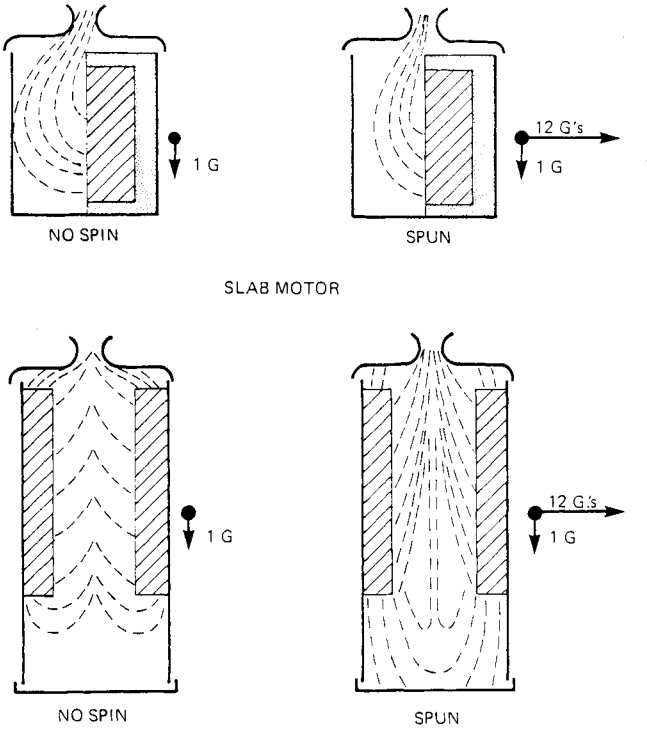


Fig. 7 Trajectories of representative particles in slab motor and in 127-mm (5-in.) CP.

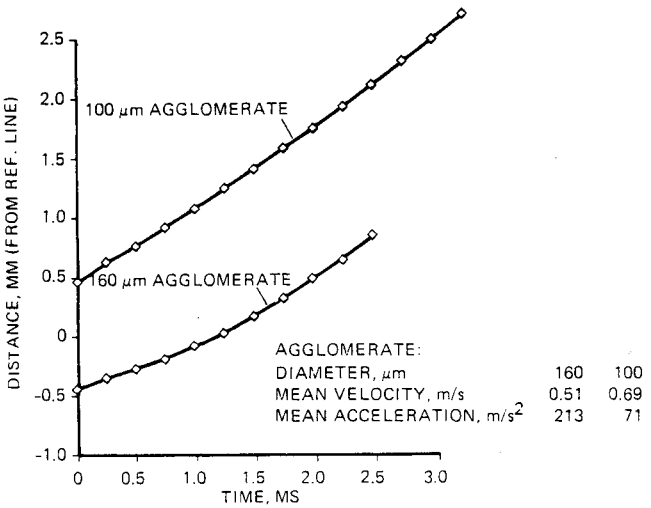


**Fig. 8 Examples of particle displacement vs time under cross flow conditions.**

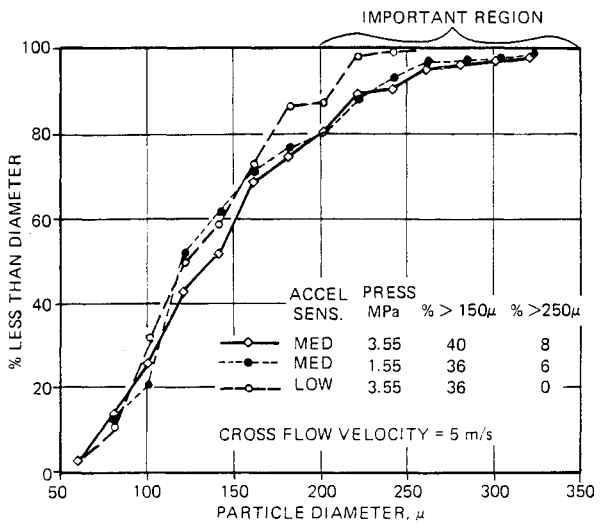


**Fig. 9 Agglomerate distribution showing significance of small percentage of the larger agglomerates.**

combustion chamber and one-dimensional flow approximations along the port. The drag force on the burning agglomerates was approximated as follows:

$$F = 0.5 C_D \rho_g (u - u_{ag})^2 (\pi/4) d_{ag}^2$$

where[22]

$$C_D = 27/Re_d^{0.84} \text{ for } Re_d \leq 80$$

A check on the consistency of the agglomerate mass (or density) and acceleration was attempted by plotting acceleration vs diameter. For conditions of constant velocity lag, the data should have correlated as $a_{ag}$ vs $d_{ag}^{-1.84}$. However, the data were not grouped well; that is, the coefficient of correlation was 0.24.

The lack of simple correlation for velocity led to an important conclusion: the agglomerate/flowfield interaction cannot be predicted by simple drag and constant particle density relationships. It is known that the agglomerate overall density is less than the density of alumina. One group of agglomerates had a density of 2.4 vs 2.7 g/cm$^3$ for alumina. But even a 2-to-1 variation in the agglomerate density would not account for the range of observed accelerations. Thus, the magnitude of the drag on an individual particle may be strongly influenced by the manner in which a particular agglomerate burns.

Since the agglomerates were burned in the flowfield and alumina smoke was discharged through the outer shell, the agglomerates may have produced nonuniformly distributed forces. During the course of the analysis, attention was given to searching for evidence of nonuniform surface forces or, in the extreme, a thrusting agglomerate. If such forces were significant, they would be revealed by erratic position-time plots. As indicated by the data and by Fig. 8, the position-time data were reasonably uniform. Thus, this study produced no evidence of large, unbalanced forces on the agglomerates in the flowfield.

Analytical procedures to predict accurately two-phase flows and agglomerate trajectories in rocket chambers are very questionable in view of the uncertainty of the agglomerate density and the apparent inconsistency of the drag relationships.

### Agglomerate Size Distributions

Analysis of the films from the cross flow window burner experiments emphasized the larger particles, mostly in the 40- to 300-μm size range. The distribution of larger particles included nearly all the aluminum mass ejected from the propellant surface. For the purpose of reducing aluminum retention in full-scale motors, attention was focused on the larger agglomerates (greater than 150 μm) since the smaller agglomerates were more readily entrained in the flowfield and discharged through the nozzle.

The diameters of the agglomerates were tabulated from the film sequences in the expectation that a statistical analysis of that data would provide useful indications of propellant behavior and slag formation in large motors (under spin conditions); that is, for a particular pressure and cross flow velocity regime, those propellants that produce a smaller mass fraction of agglomerates above a critical size should produce less slag. The diameters of at least 100 agglomerates were measured as they moved past an imaginary line about 3 mm from the leading edge of the aluminized propellant section. Thus, the moving agglomerates were taken into account. The distributions obtained from three tests are compared in Fig. 9. On first examination, the data appear very similar. However, differences in the number of larger agglomerates (greater than 150 μm) are very significant. The relatively few large agglomerates can account for the mass of the retained slag.

## Conclusion

Agglomerate formation was found to be a key process in categorizing the tendency of a propellant to form significant residue at acceleration levels of 5 to 20 $g$. Burn-rate increases due to acceleration were primarily influenced by the base burn rate without acceleration; that is, the lower burning rate propellants experienced larger burning rate increases. Al agglomeration provided only a secondary effect on burn rate, probably due to the lack of progression to long-term retention of aluminum droplets on the propellant surface. The occurrence of processes in the pockets between the larger AP particles was verified by SEM images that identified regions of high Al and Cl concentration.

Within the general class of propellants considered, slag retention was reduced by the following formulation trends: substituting larger size Al (30 μm) for very fine Al (7 μm), using HMX rather than RDX, decreasing binder level, and decreasing AP size (in the presence of significant amounts of coarse AP). The strong influences of the size of the AP on reducing agglomeration and residue were explored extensively with particularly significant results: slag retention was reduced by replacing coarse AP with fine AP and by using a more uniform AP distribution (trimodal blends instead of bimodal blends).

Particle trajectory analyses indicated that the densities of the agglomerates vary over a wide range, introducing additional uncertainties in performance predictions. However, trends of motor slag retention appeared to correlate with the number fraction of very large agglomerates (those over 250 $\mu$m).

The results of this investigation indicate that propellant performance can be improved by considering the desired motor environment in the context of the data base and by understanding the combustion mechanisms. The trends in aluminum agglomeration have been related to the processes that occur within the pockets between the larger AP particles, and attention to this zone can be used to guide formulation changes.

## Acknowledgments

The research was sponsored by the Air Force Rocket Propulsion Laboratory under Contract F04611-78-C-0055 and Thiokol IR&D projects 111-76-D001 and 111-77-D-001. A portion of the experiments were performed when the second author was with Princeton University. The contributions of Wayne E. Roe, project manager, in selecting the propellants and interpreting the data are gratefully acknowledged.

## References

[1] Price, E. W., "Combustion of Aluminum in Solid Propellant Flames," Proceedings of AGARD/PEP 53rd Meeting on Solid Rocket Motor Technology, AGARD-CP-259, 1979.

[2] Gany, A. and Caveny, L. H., "Agglomeration and Ignition Mechanisms of Aluminum Particles in Solid Propellants," *Proceedings of 17th International Symposium on Combustion*, 1978, p. 1452.

[3] Crowe, C. T. and Willoughby, P. G., "Effect of Spin on the Internal Ballistics of a Solid–Propellant Motor," AIAA Paper 66-523, 1966.

[4] Glick, R. L., Caveny, L. H., and Hodge, B. K., "Effect of Acceleration on the Burning Rate of Composite Propellants," AIAA Paper 67-470, 1967.

[5] Crowe, C. T., "A Unified Model for the Acceleration-Produced Burning Rate Augmentation of Metalized Solid Propellants," *Combustion and Science Technology*, Vol. 5, 1972, p. 55.

[6] Netzer, D. W. and Northam, G. B., "Review of the Workshop on the Effects of Acceleration on the Combustion of Solid Propellants," *10th JANNAF Combustion Meeting*, CPIA Pub. 243, Vol. I, 1973, p. 185.

[7] Mitani, T. and Niioka, T., "An Analytical Model of Solid Propellant Combustion in an Acceleration Field," *Combustion Science and Technology*, Vol. 15, 1977, p. 107.

[8] Marin, L. and Geisler, R. L., "Radial G. Force Effects on Space Propellants," *16th JANNAF Combustion Meeting*, CPIA Pub. 308, Vol. III, 1979, pp. 345-399.

[9] Northam, G. B., "Effects of Combustion on Acceleration-Induced Burning Rate Augmentation," *AIAA Journal*, Vol. 4, May 1973, p. 848.

[10] Pokhil, P. F., Belyayev, A. F., Frolov, Yu, V., Logachev, V. S., and Korotkor, A. I., "Combustion of Powdered Metals in Active Media," Nauka, Moskow, 1972, translated from Russian, in FTD-MT-24-551-73, 1973.

[11] Gany, A., Caveny, L. H., and Summerfield, M., "Aluminized Solid Propellant Burning in a Rocket Motor Flowfield," *AIAA Journal*, Vol. 16, 1978, p. 736.

[12] Micheli, P. L. and Schmidt, W. G., "Behavior of Aluminum in Solid Rocket Motors," Final Rept. AFRPL-TR-77-29, 1977.

[13] Geisler, R. L., Kinkead, S. A., and Beckman, C. W., "The Relationsip between Solid Propellant Formulation Variables and Motor Performance," AIAA Paper 75-1199, 1975.

[14] Willoughby, P. G., Baker, K. L., and Hermsen, R. W., "Photographic Study of Solid Propellants Burning in an Acceleration Environment," *Proceedings of Thirteenth Symposium (International) on Combustion*, The Combustion Institute, 1971, pp. 1033-1043.

[15] Miller, R. R., Donohue, M. T., Yount, Y. A., and Martin, J. R., "Control of Solids Distribution in HTPB Propellants," Final Rept. AFRPL-TR-78-14, 1978.

[16] Renie, J. P. and Osborn, J. R., "Temperature and Pressure Sensitivity of Aluminized Propellants," AIAA Paper 80-1166, 1980.

[17] Glick, R. L. and Condon, J. A., "Statistical Analysis of Polydisperse Heterogeneous Propellant Combustion, Steady-State," *13th JANNAF Combustion Meeting*, CPIA Pub. 281, Vol. II, 1976, p. 313.

[18] Beckstead, M. W., "A Model for Solid Propellant Combustion," *14th JANNAF Combustion Meeting*, CPIA Pub. 292, Vol. I, 1977, p. 281.

[19] Crump, J., "Combustion of Solid Propellants and Low Frequency Combustion Instability," NOTS-TP-4244, 1967.

[20] Kraeutle, K. J., "The Behavior of Aluminum during Subignition Heating and Its Dependence on Environmental Conditions and Particle Properties," *9th JANNAF Combustion Meeting*, CPIA Pub. 231, Vol. I, 1972, pp. 325-340.

[21] Gladun, V. D., Frolov, Yu. V., Kashporov, L. Ya., Shakhidzhanov, E. S., and Borisov, A. A., "Nature of Agglomeration during Combustion of Highly Metallized Condensed Systems," USSR National Academy of Sciences, Moscow, 1977.

[22] Harrje, D. T. and Reardon, F. H., (eds.), "Liquid Propellant Rocket Combustion Instability," NASA SP-194, 70, 1972.